24th COBEM - 2017

24th ABCM International Congress of Mechanical Engineering
December 3-8, 2017, Curitiba, PR, Brazil

COBEM-2017-1591
STUDY OF THE PIPE DIAMETER EFFECT ON HORIZONTAL AIR-WATER TWO-PHASE FLOW

F. Jaloretto da Silva
Department of Energy, School of Mechanical Engineering, University of Campinas – UNICAMP, Campinas, Brazil
Flow Measurement Laboratory, Institute for Technological Research of the State of São Paulo – IPT, São Paulo, Brazil
felipe.js@fem.unicamp.br
felipej@ipt.br

G. G. da Silva
Department of Energy, School of Mechanical Engineering, University of Campinas – UNICAMP, Campinas, Brazil
guilherme_silva123@live.com

S. C. Vieira
Petrobras – Petróleo Brasileiro S.A., Rio de Janeiro, RJ, Brazil
saoncv@gmail.com

C. C. Pereira
M. S. de Castro
Department of Energy, School of Mechanical Engineering, University of Campinas – UNICAMP, Campinas, Brazil
cleberdesanca@yahoo.com.br
mcastro@fem.unicamp.br

Abstract. *This study relates the influence of the pipe diameters on the flow characteristics of horizontal two-phase air-water flows at fixed length, to provide new results for multiphase flows in large diameter pipes. Steady-state experiments were ran under constant water flow rate, with 4 different pipe inner diameters (27.3 mm, 52.8 mm, 81.3 mm and 102.7 mm). Results of 81.3 and 102.7 mm i.d. showed different transition boundaries for intermittent and stratified flow patterns when compared with each pipe diameter and published studies. Moreover, data of the 27.3 and 52.8 mm i.d. showed no difference on the transition regions with early known studies. Results obtained were compared with homogeneous and separated flow models. Also, signal analysis of the differential pressure signature on time of each flow pattern were used to determine and compare the characteristics of each flow pattern on the different diameters, besides visual observation.*

Keywords: *air-water flow, two-phase flow, diameter effect, pressure drop, horizontal pipes, pressure signature*

1. INTRODUCTION

Two-phase flow is a kind of phenomenon that can be understood by the flow of two or more different states of fluid in the same conduit, such as water and water vapor, or different components flowing together, as immiscible fluids or solids dispersed in the water. The most important features of two-phase flow are the many different flow patterns occurring and its identification besides their respective pressure drop and holdup ratio. Each flow pattern has its unique relationship with measured pressure drop, fluids properties, slip between phases, void fraction and pipe dimensions. Understanding the effects on the flow pattern due to pipe dimension is important on designs, as it can be observed in many different situations like industries and science applications.

Regarding on the knowledge of two-phase flow characteristics on designing of engineering systems, especially pressure-drop and the flow pattern, many studies have already been made focusing on understand and find a kind of state of art theory for this. Mandhane *et al.* (1974), have observed that lack of single theory or correlation to predict pressure gradient. Presently, more than forty years later, Hamad *et al.* (2017) noticed the same when referring to the work of Michaelides (2006), saying that there is no general model available to predict the pressure drop within acceptable accuracy. Howsoever, there are different approaches to understand multiphase flow. Wallis (1969) distinguished the analyze by: correlations, using experimental data; simple analytic models, that do not consider the

physics details of the phenomenon but can provide some prediction; integral analyzes, considering the fluid dynamics equations and boundary conditions; and the differential analyzes, detailing velocity fields and momentum involved.

In the case of understanding the pipe diameter effect on the horizontal two-phase flow another experimental work has been made previously. The first one is the experimental study done by Kosterin (1949), who compared results from four different diameters and analyzed it with the mixture drag coefficient and Froude number. Other experimental works were done by Weisman *et al*. (1979), and Lin and Hanratty (1985). Also, on studies related to pipe diameter, Taitel and Dukler (1976) and Mandhane *et al*. (1974) are great references. One of the first studies trying to relate pressure fluctuations with flow patterns was done by Hubbard and Dukler (1966), and after by Ebner *et al*. (1987), Drahos *et al*. (1987) and Drahos (1989).

Wallis (1969) proposed the comparison of experimental data with the homogeneous model, based on a single-phase pseudo-fluid flow. Another way to compare measured pressure drop data are the two-phase flow multipliers model, by Lockhart and Martinelli (1949).

2. REVIEW OF ANALYTICAL METHODS

2.1 Homogeneous flow model

This theory provides the simplest way to model two-phase flow, which considers that both fluids has the same actual velocity. Also, mixture properties are an average of that for the fluids, and there is no slip between then. The main characteristics are calculated directly with measured data: superficial velocities (j_i), no-slip liquid holdup (λ_L), mixture density (ρ_m), mixture viscosity (μ_m) and friction factor (f_N), calculated as proposed by Hall (1957) for rough-pipe in the explicit form. Equations (1) to (5) shows the calculation methods:

$$j_i = \frac{Q_i}{A} \tag{1}$$

$$\lambda_L = \frac{j_1}{j_1 + j_2} \tag{2}$$

$$\rho_m = \rho_1 \lambda_L + \rho_2 (1 - \lambda_L) \tag{3}$$

$$\mu_m = \mu_1 \lambda_L + \mu_2 (1 - \lambda_L) \tag{4}$$

$$f_N = 0{,}001375 \left[1 + \left(20000 . \frac{\varepsilon}{d} + \frac{10^6}{\mathrm{Re}_m} \right)^{1/3} \right] \tag{5}$$

where i can be 1 or 2, indicating water and air, respectively; Re_m is the mixture Reynolds (based on the mixture properties and velocity), ε is the pipe roughness (4.6×10^{-5} m, for iron), d and A are the pipe inner diameter and area, respectively.

Finally, frictional pressure drop is calculated as shown in Eq. (6):

$$-\frac{dP}{dx} = \frac{2}{d} f_N \rho_m j^2 \tag{6}$$

2.2 Separated flow model - Lockhart-Martinelli correlations

Lockhart-Martinelli (1949) suggested a correlation of the two-phase flow pressure drop with the calculated pressure drop on the hypothesis that just one fluid was flowing in the pipe, air or water, with the same mass flow each fluid has on the two-phase flow. Based on this, there is a two-phase multiplier that can be used to determine the two-phase pressure drop. Equation (8) shows the multiplier:

$$\phi_i^2 = \left(\frac{dP}{dx} \right)_{TP} \Big/ \left(\frac{dP}{dx} \right)_{io} \tag{8}$$

and the Martinelli parameter is calculated as shown on equation (9):

$$X^2 = \left(\frac{dP}{dx}\right)_{1o} \Big/ \left(\frac{dP}{dx}\right)_{2o} = \frac{\phi_G^2}{\phi_L^2} \tag{9}$$

the index *TP* means two-phase flow, and *io* denotes just one phase: liquid or gas only.

A Blasius-type equation was used to determine the friction factor, and the pressure drop is calculated for liquid or gas only. Chisholm (1967) developed an empirical correlation to calculate the liquid phase multiplier, presented in Eq. (12).

$$C_F = a\,\mathrm{Re}_i^{-n} \tag{10}$$

Values of *a* and *n* are given on Table 1, and the Re_i is calculated with superficial velocities of each fluid, its properties and de pipe inner diameter.

Table 1. Values of *a* and *n* for each range of Reynolds value

Re_i values	**a**	**n**
Re_i<2000	16	1
2000<Re_i<100000	0.079	0.25
Re_i>100000	0,046	2

$$\left(\frac{dP}{dx}\right)_{io} = \frac{2}{d} C_F \rho_i j_i^2 \tag{11}$$

$$\phi_1^2 = 1 + \frac{C}{X} + \frac{1}{X^2} \tag{12}$$

Values of C vary depending on the values of Re_1 and Re_2, but for that case Re_i>1000 the flow is considered turbulent, and below 1000 is laminar. Table 2 shows the relations of flow type and C.

Table 2. Coefficient C values

Liquid	**Gas**	**C**
Turbulent	Turbulent	20
Laminar	Turbulent	12
Turbulent	Laminar	10
Laminar	Laminar	5

2.3 Flow pattern study by the pressure time traces and signal analyzes

Differential pressure drop signature on time were used for signal analysis of flow pattern. From them histograms of the distribution and the probability density functions (PDF) were calculated. Basically, the visual observations of the flow patterns of this study were compared with the results of signal analyzes.

Here, the histogram and PDF were calculated with a Matlab function named *ksdensity* that estimates the pdf by a kernel distribution, that is defined by a smoothing function and a bandwidth value, which control the smoothness of the resulting density curve (Matlab documentation, 2017). Calculation method are defined on equation (14).

$$\hat{f}_h(DP) = \frac{1}{nh} \sum_{i=1}^{n} K\left(\frac{DP - DP_i}{h}\right) \tag{14}$$

where DP_1, DP_2 and Dpi are random samples of differential pressure from an unknown distribution, n is the sample size, K is the Kernel smoothing function and h is the bandwidth.

3. EXPERIMENTAL FACILITIES AND PROCEDURES

The experiments were performed at the Experimental Laboratory of Petroleum (LabPetro) of the Center for Petroleum Studies (CEPETRO) at University of Campinas (UNICAMP) and at the Flow Measurement Laboratory (LV) of the Center for Mechanical, Electrical and Fluid Flow Metrology (CTMetro) at Technological Research Institute (IPT). Four setups were built, each one with different pipe inner diameters: $27.3x10^{-3}$ m (named 1"), $52.8x10^{-3}$ m (named 2"), $81.3x10^{-3}$ m (named 3") and $102.7x10^{-3}$ m (named 4") diameter. All of them were built with a fixed test section length of 12 m, resulting in experiments with 439, 227, 147 and 116 diameters of length (L/D), respectively. Pressure drop were measured with the upstream tap at 9.0 m from the test section inlet and 2.5 m apart from the downstream one. The pressure signature sensor upstream tap was at 11.8 m from the test section inlet and 0.1 m apart from the upstream one. The visualization section was installed at the end of the test section. Tap water and air were the working fluids. A schematic draw of experimental setups is shown in Fig. (1).

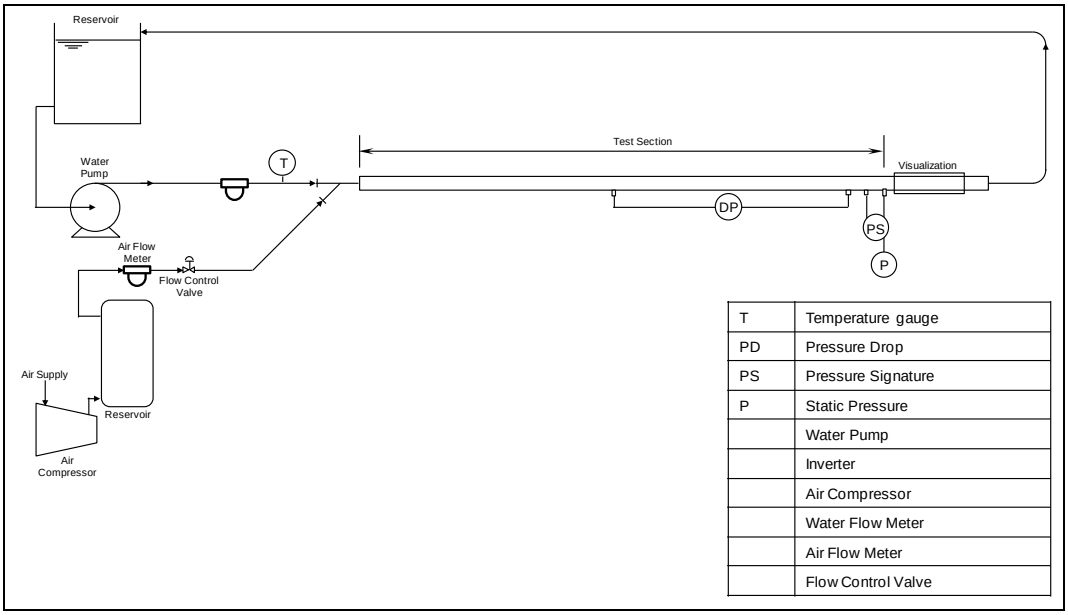

Figure 1. Scheme of the experimental setup

Flow patterns classification was done by visual observation and pressure signature signal analysis. The test procedure was made in two steps: the first one with water single-phase flow, aiming to validate the pressure sensor, and the second was the tests with two-phase air-water flows. The first step should be done every day before the two-phase flow tests to validate the results of pressure drop in comparison with established theoretical models and was named validation step. After validation, the tests with two-phase flow could get, and it was performed with a fixed water superficial velocity for which the air superficial velocity could be varied. All the superficial velocities combinations were executed three times, in ascending, descending and ascending order, with an acquisition time of about 2 minutes, to neutralize hysteresis effects and evaluate the benches repeatability, in addition to obtaining statistically relevant data.

The water flow rate was measured with two Micro Motion coriolis type, one of Model IFT9701 and the other of model DS300, and the air flow rate with a Micro Motion coriolis type model Elite CMFS015M. Pressure drop was measured with differential pressure sensors from Rosemount (model 305S), until 6000 Pa, and by a Smar sensor (model LD301) from 6000 Pa to 50 kPa. The reading of pressure signature time traces was made with a differential pressure drop sensor Validyne DP-15 model from -860 to 860 Pa, and with another DP-15 model from -8.6 kPa to 8.6 kPa. The static pressure was also measured by a Validyne DP-15 model sensor with a diaphragm of 550 kPa. All the Validyne sensor were each one associated with another same brand demodulator CD23 model, calibrated for each pressure range. Data acquisition were made with a NI Labview software, with a sample rate of 5 kHz, for the 3" setup, and with a sample rate of 24 kHz, with low pass filter at a 70 Hz cutoff and a 140 Hz resample, for the other three benches. Time tracing recorded are about 120 seconds, except for the 4" setup where the time recorded are about 25 seconds, and the files were after analyzed with Matlab software.

The range of superficial velocities studied for each setup is given on Table 3.

Table 3 Ranges of superficial velocities studied for each fluid and bench

Experimental Setup	Water superficial velocities (m/s)	Air superficial velocities (m/s)
0.0273 m (1”)	0.05 to 6.00	0.30 to 15.50
0.0528 m (2”)	0.05 to 2.00	0.30 to 4.75
0.0813 m (3”)	0.02 to 0.80	0.15 to 2.00
0.1027 m (4”)	0.10 to 4.00	0.15 to 1.15

4. RESULTS AND DISCUSSION

4.1 Flow Maps

As an initial understanding of the results it is important to compare the observed flow patterns in each setup and the ones predicted by literature. In all experiments only six fully developed flow patterns were observed: smooth stratified (SS), wavy stratified (SW), elongated bubbles (EB), annular (A), slug flow (SL) and bubbles (B). But not all these flow patterns had been observed in all setups. Figures (2 to 5) shows the flow pattern maps for each setup, and its possible limit regions. Only the fully developed patterns and its limits are shown.

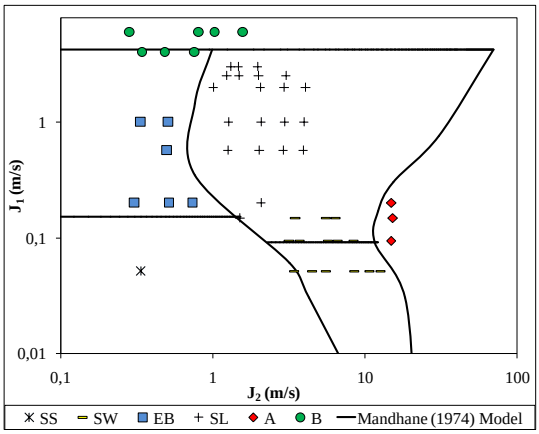

Figure 2. Flow pattern map for 1”, the curves are the flow transition boundaries proposed by Mandhane et al. (1974).

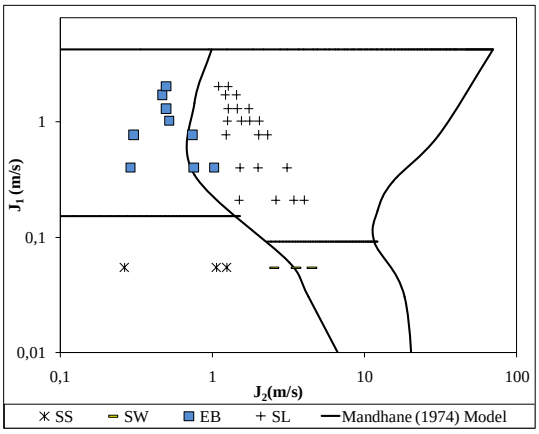

Figure 3. Flow pattern map for 2”, the curves are the flow transition boundaries proposed by Mandhane et al. (1974).

Observed transition regions for 1” and 2” have great agreement with that already mentioned by Mandhane *et al.* (1974). Except for the transition from SW to SL, at 1” diameter, it is possible to say that Mandhane et al. flow map can be used to define transitions for 1” and 2”. It is important to observe that neither annular nor dispersed bubbles flow patterns were observed at 2” setup. Furthermore, for 1” setup the transitions to annular flow pattern were observed for water superficial velocities greater than 0.3 m/s. The lines indicating transition regions on these maps are, indeed, the Mandhane's transition, except for those whose patterns were not observed on the present study.

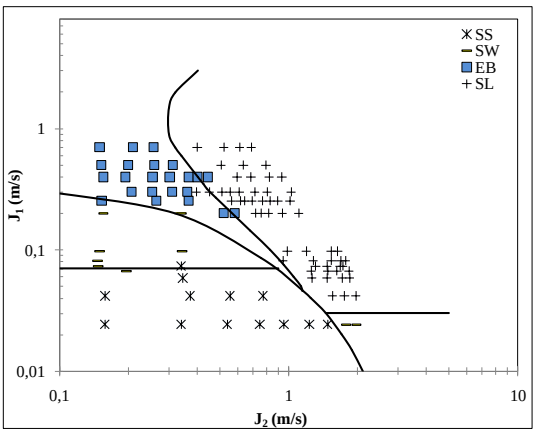

Figure 4. Flow pattern map for 3".

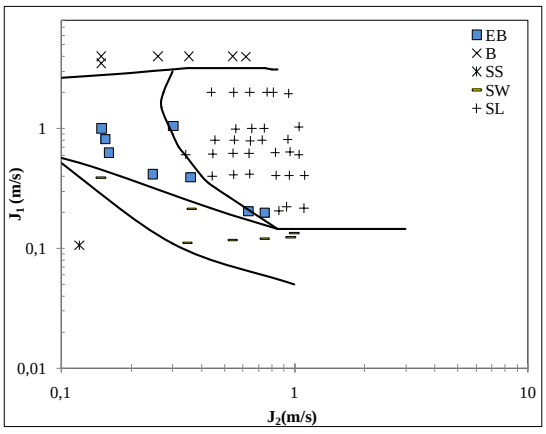

Figure 5. Flow pattern map for 4".

It could be observed that for greater diameters slug flow pattern begins at lower superficial velocities of air at all the range of water velocities. About the water superficial velocities, the beginning of slug flow for the 3" setup is at lower water superficial velocities than for the 4", and even for 2" and 1" setups. Also, the transition from SW to SL is shifted down for the 3" diameter setup.

There are, for the highest diameters (3" and 4"), the presence of the SW flow pattern region between SS and EB, which did not occurred for the lowest diameters (1" and 2"). Results for transition to B are under the prediction of Mandhane's work.

4.2 Pressure Drop

About the pressure drop measurements, the data is presented compared with predictions from Homogeneous and Separated Phases models in Figs. (6 and 7), for 1" and 4" setups, respectively.

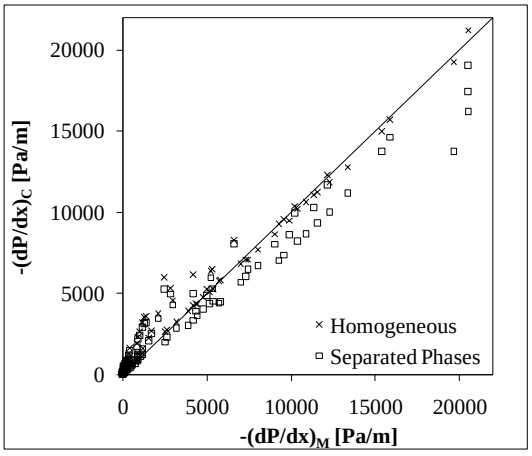

Figure 6. Comparative of Homogeneous and Separated Phases model results for 1" setup.

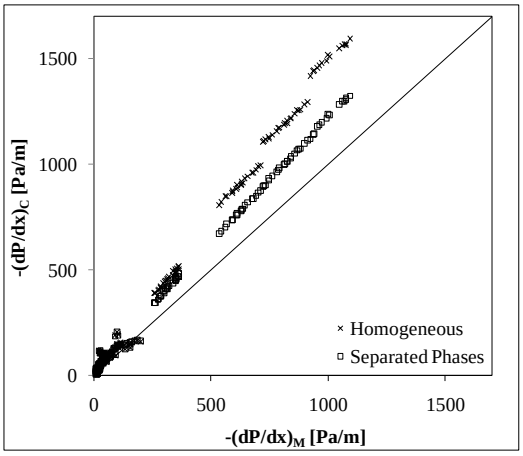

Figure 7. Comparative of Homogeneous and Separated Phases model results for 4" setup.

Neither the Homogeneous nor the Separated Phases Model showed good agreement with the experimental data as expected. Since there is a large range of fluids velocities it is not expected that one simple model could get all the physics behind each flow pattern for each pipe diameter. So, there is the necessity of the usage of other models such as two-fluid or drift-flux models.

4.3 Flow Patterns

The observed fully developed flow patterns (except SS) in each setup are shown in the following figures (8 to 29), helping to understand the definition of each one at each pipe diameter.

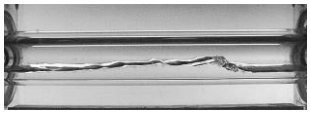

Figure 8. SW flow pattern at 1" bench, for j_1=0.10 m/s and j_2=6.62 m/s

Figure 9. EB pattern at 1" bench, for j_1=0.60 m/s and j_2=0.50 m/s, front section

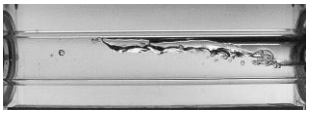

Figure 10. EB pattern at 1" bench, for j_1=0.60 m/s and j_2=0.50 m/s, rear section

Figure 11. SL pattern at 1" bench, for j_1=1.00 m/s and j_2=2.07 m/s, front section

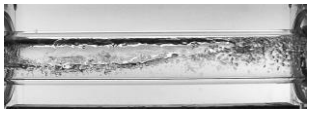

Figure 12. SL pattern at 1" bench, for j_1=1.00 m/s and j_2=2.07 m/s, rear section

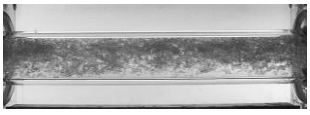

Figure 13. B flow pattern at 1" bench, for j_1=6.00 m/s and j_2=1.57 m/s

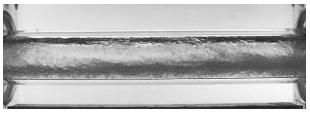

Figure 14. A flow pattern at 1" bench, for j_1=0.60 m/s and j_2=12.94 m/s

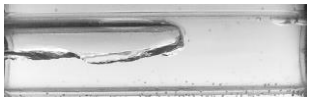

Figure 15. EB pattern at 2" bench, for j_1=0.15 m/s and j_2=0.46 m/s, front section

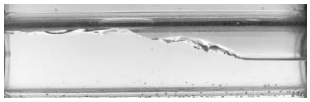

Figure 16. EB pattern at 2" bench, for j_1=0.15 m/s and j_2=0.46 m/s, rear section

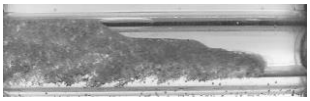

Figure 17. SL pattern at 2" bench, for j_1=0.15 m/s and j_2=2.99 m/s, front section

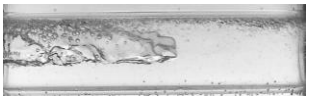

Figure 18. SL flow pattern at 2", j_1=0.15 m/s, j_2=2.99 m/s, rear section

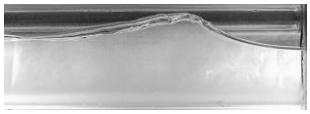

Figure 19. SW flow pattern at 3" bench, for j_1=0.07 m/s and j_2=0.20 m/s

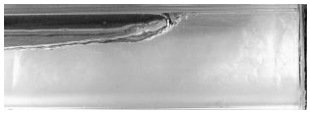

Figure 20. EB pattern at 3" bench, for j_1=0.30 m/s and j_2=0.25 m/s, front section

Figure 21. EB pattern at 3" bench, for j_1=0.30 m/s and j_2=0.25 m/s, rear section

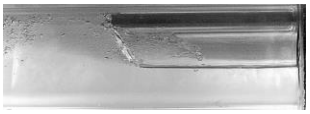

Figure 22. SL pattern at 3" bench, for j_1=0.10 m/s and j_2=1.54 m/s, front section

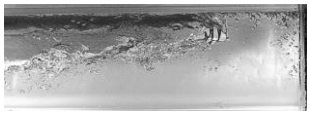

Figure 23. SL pattern at 3" bench, for j_1=0.10 m/s and j_2=1.54 m/s, rear section

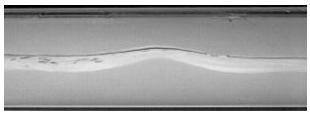

Figure 24. SW flow pattern at 4" bench, for j_1=0.22 m/s and j_2=0.55 m/s

Figure 25. EB pattern at 4" bench, for j_1=0.39 m/s and j_2=0.36 m/s, front section

Figure 26. EB pattern at 4" bench, for j_1=0.39 m/s and j_2=0.36 m/s, rear section

Figure 27. SL pattern at 4" bench, for j_1=0.62 m/s and j_2=0.55 m/s, front section

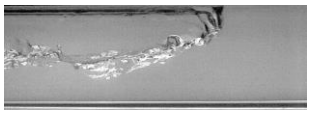

Figure 28. SL pattern at 4" bench, for j_1=0.62 m/s and j_2=0.55 m/s, rear section

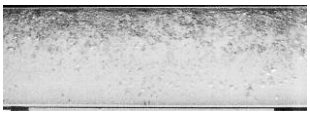

Figure 29. B flow pattern at 4" bench, for j_1=3.99 m/s and j_2=0.26 m/s

4.4 Pressure Signature Data Analysis

Now focusing on flow pattern identification using pressure time traces, or pressure signature, typical signals of each pattern will be presented, as they were visually identified the comparison can be done directly. In conjunction with the time signature graphs, the statistical behavior through the histogram of the data and its probability density function (PDF) will also be evaluated.

For smooth stratified pattern, it is possible to notice pressure oscillation of lower intensity, with peaks at low values, since the pressure gradient value for this flow pattern is very small. Sometimes, after a long time stabilized, a slug, or some wave, could pass on test section and it was considered as a characteristic on the setup itself. Figure 30 shows time traces for all four setups at SS flow pattern.

For probability density functions of SS it was observed that the histogram profile resembles the normal distribution, but the tail of both sides of the curve is quite extensive. Information like symmetry and distribution shape, here presented with skewness (s) and kurtosis (k) values, shall be useful on distinguish the patterns. Figure 31 presents this information.

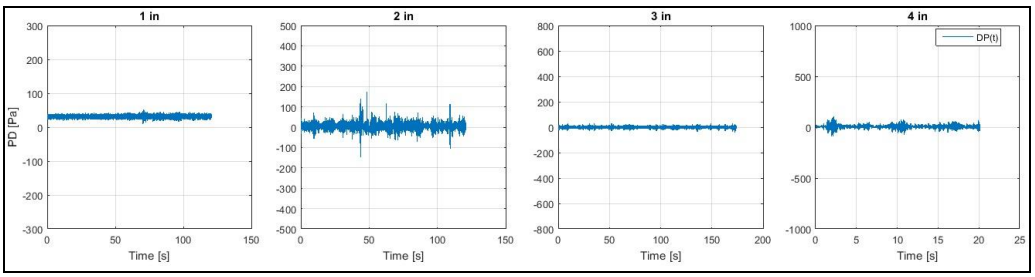

Figure 30. Time traces of differential pressure at SS pattern, for all setups.

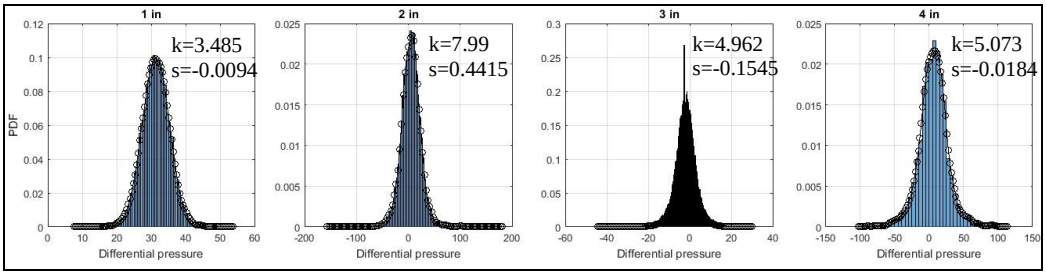

Figure 31. PDF curves at SS pattern, for all setups

When the flow pattern is SW pressure variations become common and some intermittency becomes clearer. Its PDF distributions have not changed significantly from the SS analysis, and the tails are also quite extensive. The time traces and calculated PDF for each signal at SW pattern are given in Fig. (32).

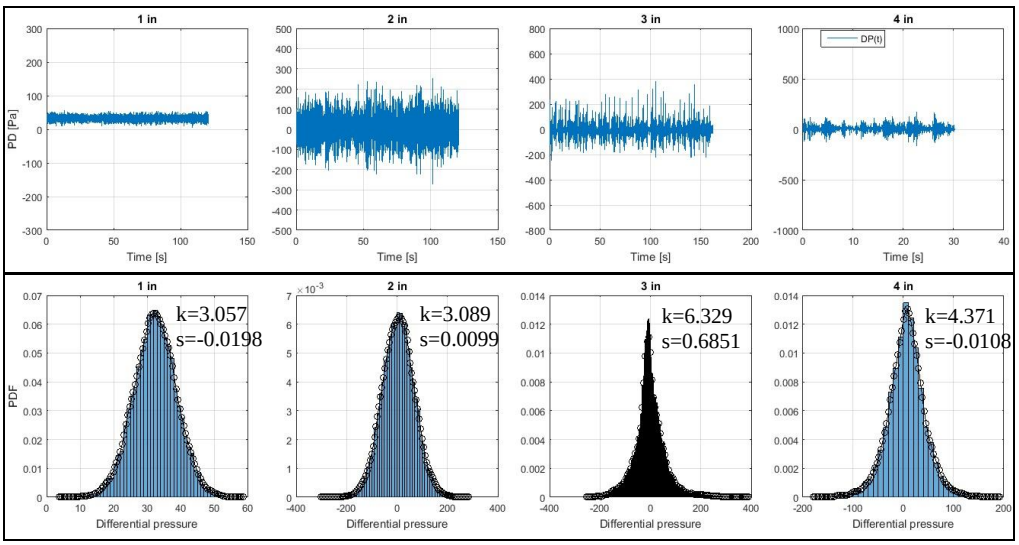

Figure 32. Time traces and PDF curves of differential pressure at SW pattern, for all setups.

For EB pattern one can clearly see the characteristic intermittency. And the PDF curves showing the difference noted on time traces. Because of intermittence distribution seems to be thinner. Figure (33) gives the plots.

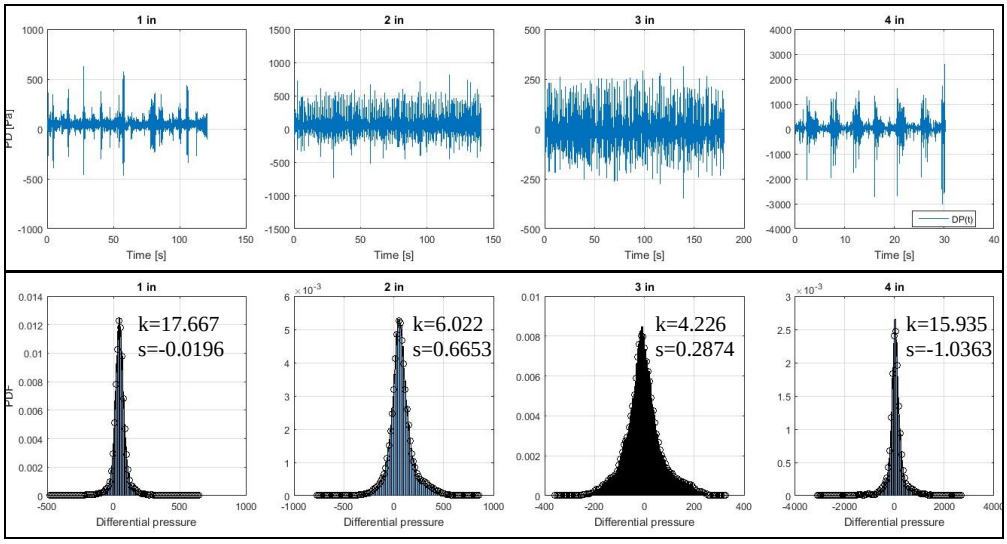

Figure 33. Time traces and PDF curves of differential pressure at EB pattern, for all setups.

Following, are the results for SL pattern. The slug flow pattern is marked by a clear indication of intermittence, with high values of pressure peaks. This flow pattern has the narrowest PDF curve among all observed patterns. It is possible to understand why observing the time traces, there are about three different pressure levels measured: maximum and minimum peaks besides around zero values. Most of values are around zero with intermittent less common peaks. Figure (34) shows this graphically.

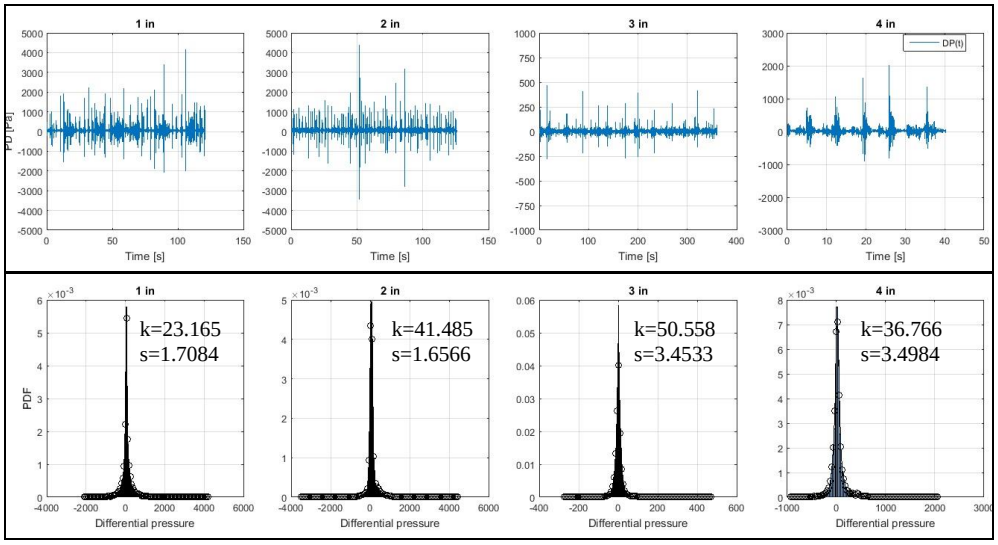

Figure 34. Time traces and PDF curves of differential pressure at SL pattern, for all setups.

The flow pattern bubble, on fig. (35), was observed just for 4” and 1” setups. At this flow pattern the pressure oscillation does not show clear intermittence, however there is high variation in the differential, since the tube is completely filled with liquid in which the air is present in small bubbles. These bubbles generate the identified oscillations. It is important to note the high level of pressure oscillation.

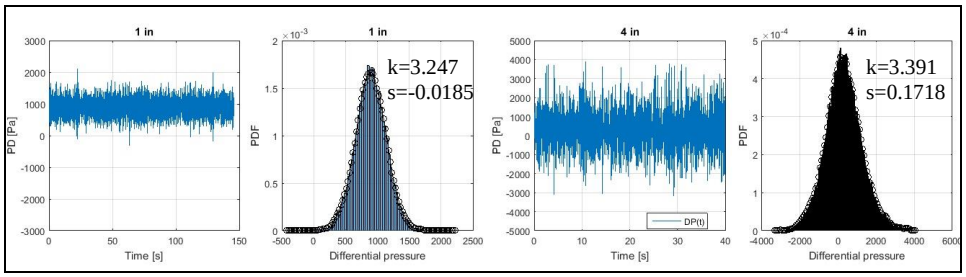

Figure 35. Time traces and PDF curves of differential pressure at B pattern, for 1" and 4" setups.

The last flow pattern, annular, was observed just for 1” setup. In the annular flow pattern the variation of the differential pressure is very similar to SS, but with a high amplitude of the peaks. The PDF plot shows some similarity with the SS one, for 1” bench, but together with time trace the pattern is different from that one. Figure (36) shows both plots.

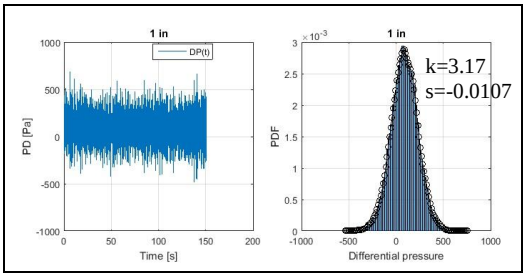

Figure 36. Time traces and PDF of differential pressure at A pattern, for 1” setup.

There is a lot of hidden information in the pressure signature of each flow pattern. A deeper analysis could show the characteristic frequencies of each flow pattern and so on, if there is some impact of the pipe diameter in this analysis. This will be object of further works.

5. CONCLUSIONS

The experiments made possible the construction of a more detailed flow regime map for air-water two-phase flow on horizontal pipes of several diameters. This has given new information about flow pattern transition regions for large diameter pipes. Furthermore, values measured and calculated for pressure drop had shown that neither the homogeneous nor the separated phases model give acceptable predictions on estimating theoretical values Although homogeneous model had shown good agreement with the results for 1" setup, this does not happen with the others.

Data for the studied pressure signature suggests a strong possibility on determining the flow pattern analyzing time trace together with probability functions. Comparisons with observed patterns reinforce this possibility, and this kind of analyze can be used for predicting flow pattern in online applications.

6. ACKNOWLEDGEMENTS

The authors would like to acknowledge IPT, ALFA Research Group and all of its contributors for the support and suggestions.

7. REFERENCES

Drahos, J., and Cermák, J., 1989. "Diagnostics of gas-liquid flow patterns in chemical engineering systems". In *Chemical Engineering and Processing: Process Intensification*, Vol. 26, No. 2, p. 147-164.

Drahos, J., Cermák, J., Selucký, K., and Ebner, L., 1987. "Characterization of hydrodynamic regimes in horizontal two-phase flow: Part II: Analysis of wall pressure fluctuactions." In *Chemical Engineering and Processing: Process Intensification*, Vol. 22, No. 1, p. 45-52.

Ebner, L., Drahos, J., Ebner, G., and Cermák, J., 1987. "Characterization of hydrodynamic regimes in horizontal two-phase flow: Part I: Pressure drop measurements." In *Chemical Engineering and Processing: Process Intensification*, Vol. 22, No. 1, p. 39-43.

Hall, N.A., 1957. *Thermodynamics of Fluid Flow*, Longmans Green, New York City.

Hamad, F.A., Faraji, F., Santim, C.G.S., Basha, N., and Ali, Z, 2017. "Investigation of pressure drop in horizontal pipes with different diameters". In *Int. J. Multiphase Flow*, Vol. 91, p. 120-129.

Hubbard, M. G., and Dukler, A. E., 1966. "The Characterization of Flow Regimes for Horizontal Two-Phase Flow". In *Proceedings of the Heat Transfer and Fluid Mechanics Institute*, p. 101-121.

Kosterin, S. I., 1949. "An investigation of the influence of the diameter and inclination on the hydraulic resistance and flow structure in gas-liquid mixtures". In *Izv.Akad.Nauk SSSR. OTN* , Vol. 12., p. 1824-1830.

Lin, P.Y., and Hanratty, T.J., 1987. "Effect of pipe diameter on flow patterns for air-water flow in horizontal pipes". In *Int. J. Multiphase Flow*, Vol. 13, p. 549-563.

Lockhart, R.W. and Martinelli, R.C., 1949. "Proposed correlation of data for isothermal two-phase, two-component flow in pipes". In *Chem. Eng. Prog*, Vol. 45, No. 1, p. 39-48.

Mandhane, J.M., Gregory, G.A., and Aziz, K., 1974. "A flow pattern map for gas-liquid flow in horizontal pipes". In *Int. J. Multiphase Flow*, Vol. 1, p. 537-553.

MathWorks Documentation, 2017. "ksdensity: Kernel smoothing function estimate for univariate and bivariate data". 3 Oct. 2017 < https://www.mathworks.com/help/stats/ksdensity.html>.

Michaelides, E.E., 2006. *Particles, bubbles and drops - their motion, heat and mass transfer*. World Scientific Publishers, New Jersey.

Taitel, Y. and Dukler, A. E., 1976. "A Model for Predicting Flow Regime Transition in Horizontal and Near Horizontal Gas-Liquid Flow". In *AIChE J.*, Vol. 22, No. 1, p. 47-55.

Wallis, G.B., 1969. *One dimensional two-phase flow*. McGraw-Hill Book Co. Inc., New York City.

Weisman, J., Duncan, D., Gibson, J., and Crawford, T., 1979. "Effect of fluid properties and pipe diameter on two-phase flow pattern in horizontal lines". In *Int. J. Multiphase Flow*, Vol. 5, p. 437-462.

8. RESPONSIBILITY NOTICE

The authors are the only responsible for the printed material included in this paper.